

A Recruitment Model of Quasi-Linear Power-Law Stress Adaptation in Lung Tissue

JASON H. T. BATES

Department of Medicine, University of Vermont College of Medicine, HSRF 228149 Beaumont Avenue, Burlington, Vermont 05405-0075, USA

(Received 15 March 2006; accepted 1 March 2007; published online 23 March 2007)

Abstract—When lung tissue is subjected to a step in strain, it exhibits a stress adaptation profile that is a power function of time. Furthermore, this power function is independent of the strain, even though the quasi-static stress–strain relationship of the tissue is highly nonlinear. Such behavior is known as quasi-linear viscoelasticity, but its mechanistic basis is unknown. We describe a model of soft tissue rheology based on the sequential recruitment of Maxwell bodies. The model is homogeneous in its elemental constitutive properties, yet predicts both power-law stress relaxation and quasi-linear viscoelasticity even when the stress–strain behavior of the model is nonlinear. The model suggests that stress relaxation in lung tissue could occur via a sequence of micro-rips that cause stresses to be passed from one local stress bearing region to another.

Keywords—Soft tissue rheology, Maxwell body, Recruitment, Stress–strain curve.

INTRODUCTION

Lung parenchyma is viscoelastic; the energy imparted to it during stretch is initially stored elastically but becomes dissipated over time as the micro-structural elements of the tissue gradually rearrange themselves toward a state of lower global energy. This process is known as stress relaxation and is conventionally modeled using constructs containing one or more Maxwell bodies,^{11,12} which are elastic springs connected to resistive dashpots (Fig. 1). For a single Maxwell body having constant dashpot resistance (R) and spring constant (E), the decay in stress following a step increase in strain is exponential with time-constant R/E . However, when a strip of pre-conditioned lung tissue is subjected to a sudden step in strain, the log-

arithm of stress relative to initial stress (S), plotted against the logarithm of time (t) describes an almost perfect straight line over many decades of t .^{6,15,31} In other words,

$$S = At^{-k} \quad (1)$$

where k is some positive constant and A is a (usually nonlinear) function of the static stress–strain properties of the tissue. Equivalently, the magnitude of the mechanical impedance of such tissue is a power function of frequency.^{6,10}

Collections of Maxwell bodies, such as shown in Fig. 1, will exhibit power-law stress relaxation if their respective time-constants are distributed hyperbolically.¹¹ However, this seems too contrived given that power laws are found to describe the stress relaxation of other biological soft tissues,⁸ and indeed appear ubiquitously throughout nature in general.¹ It seems unlikely we should have to account for the genesis of power laws in terms of one particular type of time-constant distribution. Conventional Maxwell body models also run into difficulties when they try to account for the nonlinear rheological behavior of lung parenchyma, which exhibits the curious attribute of being confined to the tissue's static stress–strain properties.^{9,12,20,31} Fung called this phenomenon quasi-linear viscoelasticity,^{11,12} yet its mechanistic basis remains obscure.

Thus, even though conventional Maxwell body models may be useful as empirical descriptors, they apparently fail to capture some key aspect of the underlying physics that leads to the progressive relief of stress within lung parenchymal tissue. Here, we describe a model based on a novel arrangement of Maxwell bodies that allows them to be recruited sequentially in order to relax stress. This model predicts both the power-law stress relaxation and quasi-linear viscoelasticity that has been observed experimentally in lung tissue strips.⁶

Address correspondence to Jason H. T. Bates, Department of Medicine, University of Vermont College of Medicine, HSRF 228149 Beaumont Avenue, Burlington, Vermont 05405-0075, USA. Electronic mail: jason.h.bates@uvm.edu

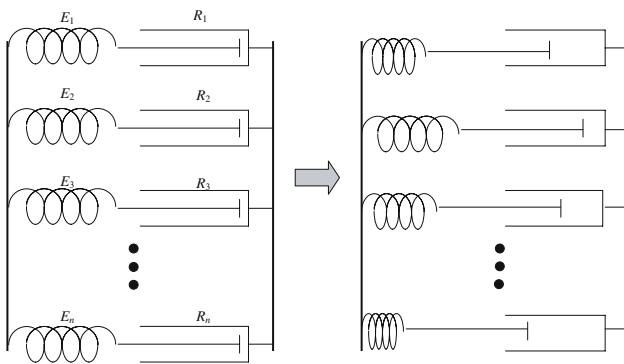


FIGURE 1. A conventional viscoelastic model consisting of n Maxwell bodies arranged in parallel. Immediately following a step in strain, shown on the left, the dashpots (resistances R_1, R_2, \dots, R_n) are all fully compressed while the springs (stiffnesses E_1, E_2, \dots, E_n) are all equally extended. Some time later, shown on the right, the springs are at various stages of decompression according to their relative time constants (the ratios R_i/E_i).

THEORY

The Genesis of Power-Law Behavior

To address the issue of why stress relaxation in lung tissue should follow a power law, as opposed to any other monotonically decreasing function of time, we first note that power laws abound throughout the natural world and are thought to reflect some general property of dynamic complexity.^{1,3} The appearance of a power law in stress adaptation, which is obviously a dynamic and complex process, is therefore not entirely surprising. What is not clear, however, is why the power law, as opposed to any other functional form, is the preferred signature of a complex system. This issue has puzzled the scientific community for decades, and a number of explanations have been proposed. For example, West³⁰ suggested that what we often take to be a power law distribution for the probability of some event may actually be the tail of a log-normal distribution, which rivals the Gaussian distribution in its ubiquity. The log-normal distribution results when the stochastic event in question is the end result of a cascade of necessary prior stochastic events, a mechanism which certainly has the appropriate level of generality required of an explanation for power law behavior. The log-normal distribution is quadratic rather than straight in a log-log plot, but the right-hand tail of such a plot can still appear remarkably straight over an extended range on log-log axes, particularly when the variance of the distribution is large.

Another theory for the genesis of power law behavior is self-organized criticality,^{1,2} which holds that when a complex dynamic system receives a continual supply of some currency (be it energy, matter, stress, or whatever), the currency will tend to become

internally organized near a critical state that poises the system on the brink of stability. Further supply will push the system beyond the stable limit, causing an avalanche of currency redistribution that re-establishes the near-critical state again. The archetypal example of self-organized criticality is the sandpile created by steadily dropping grains of sand onto a surface until the sides of the pile achieve a critical slope. Further addition of sand to the center of the pile will then trigger avalanches that slide down the sides of the pile, causing the base of the pile to expand while maintaining the sides at the same critical slope. Computational and experimental models have shown that the size and timing of avalanches off the sandpile follow power-law probability distributions.¹

Yet another source of power-law behavior that has recently received much attention is the “rich-get-richer” mechanism suggested to be behind the evolution of hubs in the internet.^{3,4} The idea here is that a small number of internet sites, for one reason or another, gain an unusual amount of early success which feeds on itself to increase their notoriety in ever increasing amounts. Most sites, meanwhile, continue to languish in relative obscurity. Barabasi and co-workers^{3,4} developed a model of the internet that combines the rich-get-richer mechanism with probabilistic network growth. This model produces asymptotic power-law behavior¹⁸ and may explain why such behavior seems to characterize all manner of complex dynamic networks.³

The common thread running through all the above theories for the genesis of power laws is what might be termed *sequentiality*. That is, the appearance of the stochastic event in question is attributed to a sequence of necessary antecedent events. Furthermore, each antecedent event has its own probability of occurring once given the chance, and must reach completion before the next event in line is initiated. For example, when a system becomes self-organized to the critical state, a little extra push on one of the system components causes it to exceed its yield threshold and push on its neighbor, which then exceeds its own threshold, and so on. Similarly, to get really rich in the rich-get-richer model it is necessary to be already pretty rich, which itself requires being a little bit rich, and so on, so that attaining a certain level of richness requires that lower levels of richness be attained first. These considerations suggest that sequentiality may also be the key to modeling power-law stress adaptation.

Sequentiality is not, however, a feature of conventional models of tissue stress adaptation in which collections of Maxwell bodies are arranged either in series or parallel. Consider, for example, the parallel collection of Maxwell bodies at the left-hand side of Fig. 1, shown immediately after a step in strain. All

the dashpots are fully compressed and all the springs are equally stretched. Subsequently, these Maxwell bodies relax at different rates so that at any later point in time their springs are at various stages of decompression, such as the situation shown at the right-hand side of Fig. 1. Nevertheless, all Maxwell bodies continue to bear at least some of the total stress across the model at all times, rather than taking turns one at a time. The same also applies when the Maxwell bodies are arranged in series. If sequentiality is indeed the key to power-law behavior, then to simulate power-law stress adaptation we require a model whose elements contribute to the system dynamics in sequence rather than simultaneously.

Stress Relaxation Through Sequential Recruitment of Elastic Elements

The problem with conventional models of stress adaptation, in terms of their lack of sequentiality, is not with Maxwell bodies themselves but rather with how they are arranged. It is possible, however, to construct a model based on Maxwell bodies that does exhibit sequentiality provided one also invokes the notion that dashpots are not simply resistors that resist movement indefinitely. Instead, we need to think of dashpots as models of physical pistons sliding inside cylinders, which can only elongate a finite amount before the piston slides out of the cylinder and the two components separate. Consider a single Maxwell body that bears the entire stress induced by a step increase in strain, and therefore also accounts for all the initial dynamics of stress relaxation (Fig. 2, left-hand side). Let the dashpot of this Maxwell body have a short length of travel so that its associated spring can only contract a small amount before the two moving parts of the dashpot disengage. Further, let the spring have a negligible resting length, so that when the dashpot piston slides out of its cylinder the two components will fly apart as the spring retracts. To prevent the model from losing its integrity entirely at this point, connect a second Maxwell body between the piston of the first dashpot and the right-hand support of the model. Provided the length of the first dashpot is small enough, the second spring will have achieved only negligible extension by the time the first dashpot separates. Following separation, however, the spring of the second Maxwell body becomes extended so as to share the total extension equally with the first spring (Fig. 2, right-hand side). However, because the extension of each spring is half the original extension of the first spring, the stress across the model is also commensurately lower. Stress relaxation continues to occur, but now it is the piston of the second dashpot

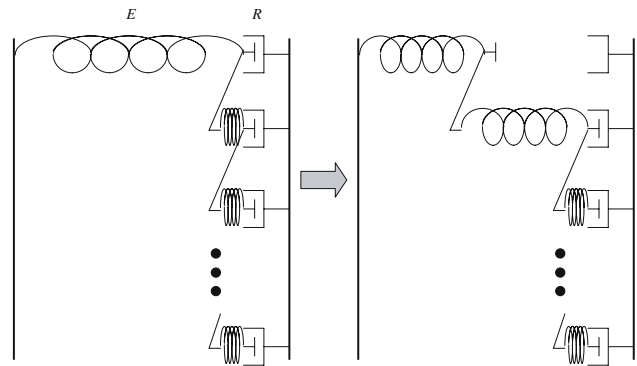


FIGURE 2. A novel model of stress adaptation involving the sequential recruitment of Maxwell bodies. Immediately following a step in strain, the entire stress across the model is born by a single spring, as shown on the left. After decompressing a short distance, the piston of the dashpot connected to this spring disengages from its cylinder, and a second spring is recruited to share the strain with the first spring, as shown on the right. This process continues as ever more springs are recruited to share the strain and transmit the stress. All springs have the same stiffness, E , and all dashpots have the same resistance, R .

that is doing the sliding, until it too reaches the end of its travel and disengages. A third Maxwell body then comes into play, reducing the common spring stress even further, and so on. In this way, the task of adapting to the stress across the model is passed in turn from one Maxwell body to the next, each time with a sudden reduction in stress as a new spring is recruited to share the total extension. The model in Fig. 2 thus has the characteristic of sequentiality we identified above as being central to systems exhibiting power-law behavior.

We now demonstrate that the tension in this model relaxes according to Eq. (1). Let the elastic behavior of each spring be given by

$$S = E\Delta x^\alpha \quad (2)$$

where E is an elastic constant, Δx is the extension of the spring beyond its unstressed length, and α is a constant. When α is 1 the spring is Hookean, but arbitrary degrees of strain stiffening (typical of biological tissue) are permitted by increasing the value of α above unity. Suppose we represent a length of tissue as N identical springs connected in series. If the tissue is stretched beyond its unstressed length by an amount L , then the extension of each individual spring is L/N and the common stress is

$$S = E\left(\frac{L}{N}\right)^\alpha \quad (3)$$

When an additional spring becomes recruited into the line of stress-bearing elements by the mechanism

illustrated in Fig. 2, the total strain remains at L , but this is now shared equally by $N + 1$ springs each with extension $L/(N + 1)$. Invoking the binomial theorem, we find the change in S produced by this recruitment to be

$$\begin{aligned} \Delta S &= E\left(\frac{L}{N+1}\right)^\alpha - E\left(\frac{L}{N}\right)^\alpha \\ &= E\left(\frac{L}{N}\right)^\alpha \left[\left(1 + \frac{1}{N}\right)^{-\alpha} - 1 \right] \\ &= E\left(\frac{L}{N}\right)^\alpha \left[\frac{-\alpha}{N} + \frac{\alpha(\alpha+1)}{2!N^2} - \dots \right] \end{aligned} \tag{4}$$

If N is large, as would be the case for a macroscopic tissue strip when each spring represents a micro-constituent of the tissue, then

$$\begin{aligned} \Delta S &\approx -\frac{\alpha E}{N} \left(\frac{L}{N}\right)^\alpha \\ &= -\frac{\alpha}{LE^{\frac{1}{2}}} \left[E\left(\frac{L}{N}\right)^\alpha \right]^{\frac{\alpha+1}{\alpha}} \\ &= -\frac{\alpha}{LE^{\frac{1}{2}}} S^{1+\frac{1}{\alpha}} \end{aligned} \tag{5}$$

Next, we need an expression for the time taken to relax stress by the amount given in Eq. (5). If the dashpots have a sufficiently short length of travel, D , then S remains essentially constant during the movement of each dashpot. The speed of movement, v , is inversely related to the dashpot resistance. So as not to be constrained by the requirement that this resistance be independent of velocity we will let the resistive force generated within the dashpot as it moves be proportional to v raised to some power β . That is,

$$Rv^\beta = S \tag{6}$$

But

$$v \approx \frac{D}{\Delta t} \tag{7}$$

where Δt is the time taken for the piston of the dashpot to move its full length of travel. Therefore,

$$\Delta t = DR^{\frac{1}{\beta}} S^{-\frac{1}{\beta}} \tag{8}$$

In the limit of continuity, this gives, from Eqs. (5) and (8),

$$\frac{\Delta S}{\Delta t} \rightarrow \frac{dS}{dt} = -\frac{\alpha}{LE^{\frac{1}{2}}DR^{\frac{1}{\beta}}} S^{1+\frac{1}{\alpha}+\frac{1}{\beta}} \tag{9}$$

Solving this differential equation gives

$$\begin{aligned} \int_{S_0}^S -\frac{LE^{\frac{1}{2}}DR^{\frac{1}{\beta}}}{\alpha} S^{-(1+\frac{1}{\alpha}+\frac{1}{\beta})} dS &= \left[\frac{\beta LE^{\frac{1}{2}}DR^{\frac{1}{\beta}}}{\alpha+\beta} S^{-(\frac{1}{\alpha}+\frac{1}{\beta})} \right]_{S_0}^S \\ &= \frac{\beta LE^{\frac{1}{2}}DR^{\frac{1}{\beta}}}{\alpha+\beta} S^{-(\frac{1}{\alpha}+\frac{1}{\beta})} - \frac{\beta LE^{\frac{1}{2}}DR^{\frac{1}{\beta}}}{\alpha+\beta} S_0^{-(\frac{1}{\alpha}+\frac{1}{\beta})} \\ &= \frac{\beta LE^{\frac{1}{2}}DR^{\frac{1}{\beta}}}{\alpha+\beta} S^{-(\frac{1}{\alpha}+\frac{1}{\beta})} - \frac{\beta L^{-\frac{\alpha}{\beta}} E^{-\frac{1}{\beta}} DR^{\frac{1}{\beta}}}{\alpha+\beta} N_0^{(1+\frac{\alpha}{\beta})} \\ &= \int_0^t dt \\ &= t \end{aligned} \tag{10}$$

where N_0 is the initial number of springs that bear the initial stress S_0 , and we used Eq. (3) to define S_0 . Rearranging Eq. (10) gives

$$S = \left(\frac{\beta LE^{\frac{1}{2}}DR^{\frac{1}{\beta}}}{\alpha+\beta} \right)^{\frac{(\frac{\alpha\beta}{\alpha+\beta})}{\alpha+\beta}} \left[\frac{\beta L^{-\frac{\alpha}{\beta}} E^{-\frac{1}{\beta}} DR^{\frac{1}{\beta}} N_0^{(1+\frac{\alpha}{\beta})}}{\alpha+\beta} + t \right]^{-\frac{(\frac{\alpha\beta}{\alpha+\beta})}{\alpha+\beta}} \tag{11}$$

Equation (11) thus shows that the stress relaxation behavior of the model in Fig. 2, following a step change in strain, is a power law of t only in the asymptotic sense. That is, as t becomes large, the functional form for the stress relaxation approaches that of Eq. (1) where

$$k = \frac{\alpha\beta}{\alpha+\beta} \tag{12}$$

and

$$A = \left(\frac{\beta LE^{\frac{1}{2}}DR^{\frac{1}{\beta}}}{\alpha+\beta} \right)^{\frac{(\frac{\alpha\beta}{\alpha+\beta})}{\alpha+\beta}} \tag{13}$$

Given that power-law stress relaxation is precisely the behavior we set out to explain, this raises the question of how big t has to become in order for it to dominate $\frac{\beta L^{-\frac{\alpha}{\beta}} E^{-\frac{1}{\beta}} DR^{\frac{1}{\beta}} N_0^{(1+\frac{\alpha}{\beta})}}{\alpha+\beta}$ in Eq. (11). When this happens depends on the values of the various constants involved, most of which have so far been assigned arbitrary values. The only exceptions are that N_0 is required to be large and D is required to be small. Conveniently, we can make the quantity $\frac{\beta L^{-\frac{\alpha}{\beta}} E^{-\frac{1}{\beta}} DR^{\frac{1}{\beta}} N_0^{(1+\frac{\alpha}{\beta})}}{\alpha+\beta}$ small simply by extending these requirements to be that D is much smaller than N_0 is large. This is readily interpreted in physical terms as meaning that the length of a dashpot is small compared to the length of its associated spring

when extended. In other words, the stress relaxation profile will quickly asymptote to a power-law in t (i.e., assume the form of Eq. (1)) if the amount of stress that is relaxed by the sliding of a dashpot is negligible compared to the amount of stress that is relaxed when the next spring is recruited.

We have thus developed a simple model that exhibits power-law stress relaxation as a result of the sequential nature with which its internal stresses are passed from one dashpot to another. This is the first of the goals we set out to achieve in modeling the viscoelastic behavior of lung tissue. The other goal was to have the value of k be independent of the strain applied to the tissue, even when its static stress-behavior is highly nonlinear. Interestingly, it turns out that no further effort is required to achieve this second goal because the model in Fig. 2 already exhibits the required property. This fact is evident upon inspection of Eq. (12) which shows that k depends only on the nonlinearities associated with the stiffness of the spring (α) and the resistance of the dashpot (β) in each Maxwell body. That is, k is independent of the strain applied to the tissue. The model thus predicts that the slope of $S(t)$ in a log-log plot will always be the same regardless of the magnitude of the strain, even when the static stress-strain properties of the tissue are arbitrarily nonlinear. This behavior is characteristic of materials exhibiting quasi-linear viscoelasticity¹¹ and is precisely what is found experimentally in strips of lung tissue.⁶ The model in Fig. 2 thus exhibits the necessary qualitative behavior to be an effective representation of lung tissue viscoelasticity. The next question is whether it can explain experimental data quantitatively.

Modeling Stress Relaxation in Lung Tissue

The value of k (Eq. 1) for lung tissue strips has been observed experimentally to be about 0.045.⁶ This is achieved in Eq. (12) when β is also about 0.045 provided that α is much larger than β , which is almost certainly the case because $\alpha = 1$ if the springs in the model are Hookean, and $\alpha > 1$ if the springs exhibit strain stiffening as is seen in lung tissue.⁶ Substituting $\alpha = 3$ (to represent strain stiffening) and $\beta = 0.045$ into Eq. (13) gives

$$\begin{aligned} A &= \left(\frac{\beta LD}{\alpha + \beta} \right)^{\left(\frac{\alpha\beta}{\alpha + \beta} \right)} E^{\left(\frac{\beta}{\alpha + \beta} \right)} R^{\left(\frac{\alpha}{\alpha + \beta} \right)} \\ &= \left(\frac{\beta LD}{\alpha + \beta} \right)^{0.044} E^{0.015} R^{0.99} \\ &\approx R \end{aligned} \quad (14)$$

The last line of Eq. (14) was arrived at by noting that raising any quantity to a power much less than unity, such as 0.015 or 0.044, gives a result close to 1.0, while raising a quantity to a power close to unity, such as 0.99, gives a result close to the quantity itself. The model in Fig. 2 thus predicts that stress relaxation in lung tissue strips should proceed approximately as

$$S(t) \approx R t^{-\beta} \quad (15)$$

meaning that both A and k in Eq. (1) are determined only by the resistive properties of the dashpots in the model, and are essentially independent of the elastic properties of the springs.

Equation (15) also shows that, just like k in Eq. (12), A is independent of the size of the step in strain applied to the model, which differs from experimental observations on lung tissue that show A to depend markedly on strain.⁶ We therefore cannot ascribe the strain stiffening behavior of lung tissue merely to nonlinear elasticity of the springs in the model in Fig. 2. This would be naïve in any case because it is well accepted that strain stiffening of lung tissue occurs largely through the progressive recruitment of collagen fibers to bear the stress as strain increases.^{19,21} That is, lung tissue is a meshwork of collagen and elastin fibers in which, at low strain levels, most of the collagen fibers are wavy or crimped, and consequently are under little tension, while the elastin fibers carry the stress. As strain increases, progressively more collagen fibers become straightened and take over the stress-bearing role from their associated elastic fibers. Collagen is much stiffer than elastin, so this gradual recruitment of collagen fibers causes a smooth progression toward an ever steeper stress-strain relationship for the tissue as a whole.

Such a recruitment mechanism is readily invoked in a model of lung tissue by considering the model in Fig. 2 to represent a local region of the collagen-elastic fiber network comprising a macroscopic sample of tissue. The tissue is then represented by numerous such constructs, each with its own unstressed length representing the strain below which the collagen fibers in the local region are flaccid. A model based on this notion is shown in Fig. 3. Multiple parallel copies of the model in Fig. 2 are connected by lengths of inextensible string to a pair of rigid members that represent the ends of a strip of lung tissue. As the rigid members move away from each other (i.e. as the tissue is strained) the strings reach their respective taut lengths, l_i , in progressive fashion. Once a string is taut, any further increases in tissue strain will cause its associated stress-adaptation unit (i.e. the model in Fig. 2) to become strained. Once this happens the spring recruitment mechanism described above will begin to occur and the stress

generated in the unit will adapt accordingly. The static stress–strain behavior of the tissue strip model is determined by the distribution of the l_i . The complete model of lung tissue is thus characterized by recruitment at two different levels, one operating within each stress adaptation unit as springs are recruited into line each time a dashpot fails, and the other operating between stress adaptation units as the length of string associated with each unit transits between flaccid and taut states.

Numerical Simulations

The model in Fig. 3 was simulated numerically as follows. At $t = 0$, we consider a series arrangement of N_0 identical springs, each with a rest length of zero and governed by Eq. (2), to be subjected to a step increase in strain of magnitude L . The subsequent movement of the dashpot connected to the final spring in the series (as per Fig. 2) is calculated using first-order Euler integration. That is, the dashpot displacement at the j th time step (x_j) is given in terms of x and S at the previous time step (x_{j-1} and S_{j-1} , respectively) by

$$x_j = x_{j-1} + \left(\frac{S_{j-1}}{R}\right)^{\frac{1}{p}} \delta t \tag{16}$$

where δt is the time step size and $x_0 = 0$. When the dashpot reaches the end of its travel (i.e. when $x = D$) its two components separate and another spring is recruited to share the internal strain, as illustrated in Fig. 2. The dashpot connected to this newly recruited spring then starts to move, beginning at $x = 0$ and proceeding until $x = D$, whereupon a further spring is

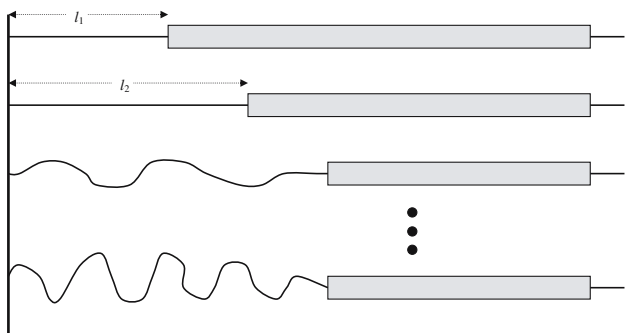


FIGURE 3. A model of a strip of lung parenchymal tissue. The two vertical supports represent the ends of the strip. The gray rectangles represent stress adaptation units that are identical versions of the model shown in Fig. 2. Each unit is connected to the left-hand support by a length of inextensible string that is unstressed when flaccid and which has a taut length $l_i, i = 1, 2, \dots$. Only those units with taut strings bear stress. As the tissue is stressed (the two vertical supports are moved away from each other) progressively more of the strings become taut and the stiffness of the entire model increases accordingly.

recruited, and so on. At each time point the stress across the model is given by

$$S_j = E \left(\frac{L - x_j}{N}\right)^\alpha \tag{17}$$

The model just described is that of a single stress adaptation unit. To simulate the complete model shown in Fig. 3, we need to have many such units connected in parallel, each with its own string length l_i . The total stress is the sum of the stresses across each unit, and is a function of the strain because units are recruited progressively as strain increases. In general, to calculate the total stress we would need to know not only how many units have been recruited, but also how much each unit had been strained. In the case of the present model, however, we have the curious situation that the stress across each unit is independent of its strain, as shown by Eq. (15). This means that all strained units carry the same stress at any point in time. Thus, all we need to know to determine the total stress is the number of units that have been recruited. Let $M(L)$ be the cumulative distribution function of units whose l_i are less than L , and which equals the number of units that have been recruited when the strain applied to the model is L . This gives the initial stress in the model as

$$S_0 = M(L)E \left(\frac{L}{N_0}\right)^\alpha \tag{18}$$

We used the above model to simulate the stress relaxation data obtained from lung tissue strips by Bates *et al.*⁶ These investigators subjected degassed strips of dog lung parenchyma to 10% step increases in length from three different initial stresses, achieved by appropriately setting the length of the tissue in each case after pre-conditioning it with a series of very slow, large amplitude, cyclic stretches. They then fit Eq. (1) to each subsequent time-course of stress, relative to its respective initial stress. To put these data in the context of the present model, we first note that lung tissue is unlikely to have truly static stress–strain properties, as it seems to exhibit dynamics over all time-scales it has been tested over.^{20,31} However, when lung tissue is pre-conditioning to a particular length, any subsequent stress adaptation at that length is very slow compared to the adaptation that occurs following a sudden stretch above the pre-conditioned length. This means that we can treat the initial tissue stresses in the experiments of Bates *et al.*⁶ as representing the stress–strain properties of a nonlinear spring connected in parallel to the sequential Maxwell elements in Fig. 2. The model in Fig. 3 is thus appropriate for simulating

the stress relaxation data of Bates *et al.*,⁶ but in order to do this we need to know what strains to apply to the model. The experimental data were obtained using 10% strains applied from three different initial stresses.⁶ Using the quasi-static stress-strain curve shown in Fig. 2 of Bates *et al.*,⁶ we estimated these strains to be in the ratio 1:1.09:1.22.

To reproduce the results of Bates *et al.*,⁶ we simulated a single stress relaxation unit (i.e. Fig. 2) starting with $N_0 = 1000$ springs and proceeding until an additional 500 springs had been recruited. We arbitrarily set the dashpot resistive constant R (Eq. 6) and the spring elastic constant E (Eq. 2) both to 1.0 (arbitrary units). The constant defining the degree of elastic nonlinearity of the model springs (Eq. 2) was arbitrarily set to $\alpha = 3$ in order to represent strain-stiffening behavior, as such behavior is what one expects to find in lung tissue. The constant defining the resistive nonlinearity of the dashpots (Eq. 6) was assigned the value determined above to be appropriate for lung tissue, namely $\beta = 0.045$. To subject the model to steps in strain of the same three relative magnitudes as the experimental strains applied to the lung tissue strips by Bates *et al.*,⁶ L was assigned the values 1.00, 1.09, and 1.22 (arbitrary units). The dashpot length D was set to the relatively very small value of 0.0001 (arbitrary units). To produce a stress dependence on strain similar to that observed experimentally by Bates *et al.*,⁶ we scaled the three simulated stress relaxation profiles according to Eq. (18), using an empirically determined choice for $M(L)$ of $0.009(e^{4.2L} - 1)$. Finally, because the relaxation rates of the dashpots in the model decrease hyperbolically as more springs are recruited, the dynamics of the model vary over an enormous range of time scale that makes the use of a single integration time step impractical. In the simulations presented here, we changed the time step as each new spring was recruited so that approximately 10 time steps were required for each new recruitment event.

When the model was run using the above sets of parameters at the three strains, we obtained the stress relaxation curves shown on log-log axes in Fig. 4(a). These curves span very large ranges of time that begin at increasingly smaller scales as the size of the step in strain increases, due to the fact that the greater initial strains cause the early spring recruitment events to occur correspondingly more rapidly. Each curve also begins with a short concave downward section corresponding to those small values of t for which the functional form of Eq. (11) does not yet approximate that of Eq. (1). Beyond these initial curvilinear portions, however, the curves become straight. We regressed the portions of these curves between 0.01 and 100 s (the time scale of the experimental data of Bates

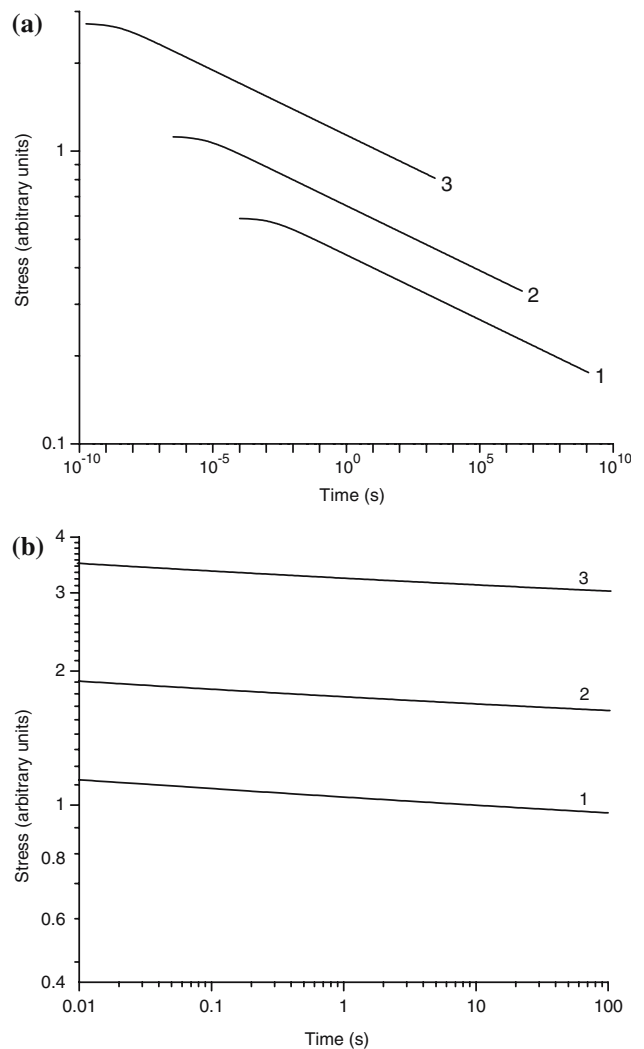


FIGURE 4. Stress relaxation profiles simulated by the model in Fig. 3. (a) Complete stress-time curves, simulated as described in the text, following strain steps of 1 (curve 1), 1.09 (curve 2), and 1.22 (curve 3). (b) The same simulated stress relaxation data presented so as to correspond to the experimental curves shown in Fig. 3 of Bates *et al.*⁶ To achieve this correspondence, initial stress values of 0.6, 1.1, and 2.1 (arbitrary units) were added to curves 1, 2, and 3 in Fig. 4(a), respectively, and replotted over the experimental time scale of 0.01–100 s.

*et al.*⁶) against t in log-log space, and obtained values for A for the three different strains of, in order of increasing strain, 0.44, 0.65, and 1.14 (arbitrary units). These lie numerically within the error limits of the corresponding values for A (in kPa) obtained by Bates *et al.*⁶ of 0.42 ± 0.05 , 0.60 ± 0.05 , and 1.25 ± 0.22 , respectively. The values of k obtained from the regressions were all 0.044, which again lie within the values found experimentally for the three increasing strains by Bates *et al.*⁶ of 0.044 ± 0.005 , 0.045 ± 0.004 , and 0.046 ± 0.006 , respectively. Finally, when values numerically equal to the initial

stresses of the three relaxation curves of Bates *et al.*⁶ (0.6, 1.1, and 2.1 kPa, respectively) are added to the corresponding simulated curves in Fig. 4(a), and the curves are plotted on log-log axes over the range $0.01 \text{ s} < t < 100 \text{ s}$, the result (Fig. 4b) is a set of negatively sloped lines that look virtually identical to the example experimental stress relaxation data plotted in Fig. 3 of Bates *et al.*⁶

DISCUSSION

A novel arrangement of Maxwell bodies has been developed in which stress is passed sequentially from one body to the next as stress relaxes (Fig. 2). There are no special distributions of constitutive properties required in this model in order for it to exhibit the required rheological properties. Indeed, all the Maxwell bodies are identical, yet the model is able to reproduce both power law stress relaxation and the separation of static nonlinear and dynamic linear behavior characteristic of quasi-linear viscoelastic materials.^{6,11} When this construct is incorporated into a distributed parallel model in which stress relaxation elements are recruited progressively with increasing strain, we are able to accurately mimic experimental data from lung tissue strips (Fig. 4). Of course, with the exception of the parameters α and β , the values of the other model parameters (E , R , L , D and N_0) were all chosen arbitrarily so as to achieve a good reproduction of the experimental data. However, these parameters merely define the operating characteristics of the model in Fig. 2, rather than corresponding to precise entities within the tissue, so what is important is their combined effect rather than their individual values. We also chose the fiber recruitment function $M(L)$ on a purely empirical basis to achieve the appropriate stress-strain behavior of the complete model in Fig. 3. Again, however, $M(L)$ is merely intended to imbue the model with appropriate macroscopic mechanical properties that arise from a strain-dependent recruitment phenomenon reminiscent in character to that known to occur in real lung tissue.¹⁹

The complete model of lung tissue thus involves recruitment at two different levels, one being at the fiber-fiber level (Fig. 3) and the other being at the level of the elastic elements within each relaxation unit (Fig. 2). Recruitment at the fiber-fiber level is based on the well accepted idea that strain stiffening in lung parenchyma occurs largely through the progressive transfer of stress from elastic fibers to collagen fibers as the latter straighten with increasing strain.²¹ However, we have yet to address the question of what the smaller scale recruitment events depicted in Fig. 2 might correspond to in real lung tissue, and how such

events could be linked to stress relaxation. The model in Fig. 2 has thus far been considered as a purely phenomenological representation of a tissue that exhibits stress relaxation. Nevertheless is it useful to think about how its novel structure may embody something about the mechanisms underlying lung tissue viscoelastic behavior. One possible interpretation of the separation of a dashpot in the model is that it represents the sudden yielding of some structure within the tissue. Suppose, for example, that lung tissue can be viewed as a web of elastic fibers embedded in a viscous ground substance. Further suppose that these fibers make contact at various points of intersection where they form temporary spot-welds capable of resisting some degree of stress, perhaps with the ground substance acting as a kind of viscous glue. In order to get the model to behave quantitatively like strips of lung tissue, we had to make β equal to 0.045. This implies that the resistive force in the dashpot is virtually independent of the velocity of the piston (Eq. 6). Although such behavior is not what one expects from a Newtonian resistance, it is precisely how a static friction element behaves.¹⁴ Polymer solutions have also been shown to exhibit a viscosity that decreases with shear rate.²⁶ Thus, the separation of a dashpot could represent the breaking of temporary static frictional contact points between fibers.

To further develop this notion, consider that the fibers in lung tissue are oriented randomly. We can then expect some of them to be taut so that their spot-welds are under tension, while other fibers are crimped or flaccid and therefore not experiencing any tension. Those spot-welds under tension would be expected to break apart over a time-scale that decreases as the tension in the tissue increases, similar to the separation of the dashpots in the model. Furthermore, when failure occurs, the fibers involved will fall away from each other, causing previously flaccid fibers and their respective spot-welds to pick up the stress at a somewhat reduced level. At a larger scale, the recruitment of a new Maxwell element in the model could represent an actual rip starting at some point within the tissue and developing as multiple components give out in a cascade of local stress failure. In any case, the central idea is that whenever a local structure within a piece of lung tissue fails, the internal stress is both reduced and passed on to neighboring structures, which themselves then become doomed to fail some time later. This mechanism may even not be limited to lung tissue. Smooth muscle exhibits length-tension plasticity that somehow seems to limit the peak force it can generate when chronically stimulated,⁵ which Speich *et al.*²⁷ attributed specifically to breakage of cross-links at the molecular level.

In the present study, we have only considered the modeling of stress relaxation. However, viscoelastic behavior of lung tissue also manifests in other characteristic ways. For example, when biological tissue, including lung parenchyma, is subjected to a constant stress it elongates continually (creeps) at an ever decreasing rate.¹¹ The model in Fig. 2, on the other hand, predicts a constant rate of creep, which is another indication that it cannot completely represent lung tissue mechanics. This problem is again solved, however, by the composite model in Fig. 3. In this model, creep under a fixed extending stress will begin rapidly because only a small number of collagen bundles are contributing to the stress relaxation. However, as the creep proceeds, progressively more collagen bundles will be recruited in parallel to share the stress, so the rate of creep will slow down accordingly.

Thus far we have only discussed the modeling of lung tissue rheology in terms of unidirectional length changes, such as those involved in creep and stress relaxation. Lung tissue also exhibits characteristic behavior during length cycling, such as stress-strain hysteresis and nonlinearity.^{20,29,31} Modeling such behavior goes beyond the scope of the present study, but presumably could be achieved in the model developed above by invoking the possibility of re-annealing of spot welds between fibers when the tissue is compressed following a stretch. Indeed, this notion was invoked by Speich *et al.*²⁷ with respect to the mechanics of smooth muscle. Re-annealing would not likely occur at exactly the same positions along each fiber in each cycle, which would result in hysteresis. Also, tissue compression would result in derecruitment of collagen fibers in the reverse of the process described above, allowing the reduced levels of stress to be re-taken up by the elastic fibers.

The model developed in this study thus suggests that stress relaxation in lung tissue may occur through a series of sudden yield events that are random and disjointed, rather than according to the usual conception of tissue constituents sliding smoothly past each other. Such a theory is still entirely hypothetical, of course, as there does not appear to be any obvious experimental evidence supporting the existence of such a mechanism during stress relaxation. Indeed, such evidence may be difficult to find if the yield events in question take place at extremely small levels of scale. For example, Mijailovich *et al.*²² modeled lung tissue dynamics as arising from slippage at micro-contact points along the lengths of adjacent fibers. Such slippage events might be extremely difficult to observe experimentally. Nevertheless, we appear to have achieved the initial goals of this study, which were to find possible mechanistic explanations for power-law stress adaptation and quasi-linear viscoelasticity. In

this regard, the model developed herein may also have relevance for other biological soft tissues that exhibit these phenomena such as cartilage,⁸ although there may be other mechanisms at play here such as fluid flow past the extracellular matrix.⁸

Finally, although the model of stress relaxation developed above was inspired by a general consideration of power-law processes that lead to the notion of sequentiality, the central role of sequentiality in the genesis of power laws has not been rigorously proven here. Indeed, the ubiquity of power law processes throughout the natural world has puzzled the scientific community for many years, so the linking of sequentiality to the production of power-laws in stress relaxation may have been purely fortuitous. Nevertheless, it is interesting to note that while the above model of lung tissue stress relaxation accounts for a power function of time, it was inspired by the sequential nature of phenomena that manifest as power-law distributions of probabilities, such as sizes of sand avalanches² and numbers of hits to an internet site.⁴ Curiously, the existence of two distinct classes of power law never seems to be made in the literature, yet they are by no means automatically equivalent because the amplitude structure of a data series is, to a large extent, independent of its sequential structure; randomly reordering the elements of a series of data points usually has a significant effect on its power spectrum but will leave its histogram unaltered.¹⁶ This suggests that sequentiality may be the common mechanism underlying phenomena exhibiting power law behavior either with respect to their amplitudes^{4,13,25,28} or their temporal structure.^{6,7,17,23,24}

In conclusion, a model of lung tissue mechanics based on the sequential recruitment of Maxwell elements has been developed. This model represents an advance over conventional models based on the Maxwell element for two reasons: (1) it exhibits power-law stress relaxation without requiring a special distribution of constitutive properties among its elements (the elements are all identical), and (2) it automatically exhibits quasi-linear viscoelastic behavior, in both qualitative and quantitative agreement with experimental data. This model suggests that stress adaptation in lung tissue may occur through sequences of discrete yield events that cause local stresses to be passed in turn from one stress-bearing region to another.

ACKNOWLEDGMENTS

This work was supported by NIH grants R01 HL075593 from the National Heart Lung and Blood Institute, and P20RR15557 from the Centers of

Biomedical Research Excellence program of the National Center for Research Resources.

REFERENCES

- ¹Bak, P. *How Nature Works. The Science of Self-Organized Criticality*. New York: Copernicus, Springer-Verlag, 1996, pp. 31–37.
- ²Bak, P., C. Tang, and K. Wiesenfeld. Self-organized criticality: an explanation of the $1/f$ noise. *Phys. Rev. Lett.* 59:381–384, 1987.
- ³Barabasi, A. L. *Linked. The New Science of Networks*. Cambridge, MA: Perseus Publishing, 2002, pp. 77.
- ⁴Barabasi, A. L., and R. Albert. Emergence of scaling in random networks. *Science* 286:509–512, 1999.
- ⁵Bates, J. H., and A. M. Lauzon. Modeling the oscillation dynamics of activated airway smooth muscle strips. *Am. J. Physiol. Lung. Cell. Mol. Physiol.* 289:L849–L855, 2005.
- ⁶Bates, J. H., G. N. Maksym, D. Navajas, and B. Suki. Lung tissue rheology and $1/f$ noise. *Ann. Biomed. Eng.* 22:674–681, 1994.
- ⁷Beard, D. A., and J. B. Bassingthwaighe. Power-law kinetics of tracer washout from physiological systems. *Ann. Biomed. Eng.* 26:775–779, 1998.
- ⁸Bischoff, J. E. Reduced parameter formulation for incorporating fiber level isoelectricity into tissue level biomechanical models. *Ann. Biomed. Eng.* 34:1164–1172, 2006.
- ⁹Doehring, T. C., E. O. Carew, and I. Vesely. The effect of strain rate on the viscoelastic response of aortic valve tissue: a direct-fit approach. *Ann. Biomed. Eng.* 32:223–232, 2004.
- ¹⁰Fabry, B., G. N. Maksym, J. P. Butler, M. Glogauer, D. Navajas, and J. J. Fredberg. Scaling the microrheology of living cells. *Phys. Rev. Lett.* 87:148102, 2001.
- ¹¹Fung, Y. C. *Biomechanics. Mechanical Properties of Living Tissues*. New York: Springer-Verlag, 1981.
- ¹²Funk, J. R., G. W. Hall, J. R. Crandall, and W. D. Pilkey. Linear and quasi-linear viscoelastic characterization of ankle ligaments. *J. Biomech. Eng.* 122:15–22, 2000.
- ¹³Gutenberg, B., and C. Richter. *Seismicity of the Earth*. Princeton: Princeton University Press, 1949.
- ¹⁴Hildebrandt, J. Pressure-volume data of cat lung interpreted by a plastoelastic, linear viscoelastic model. *J. Appl. Physiol.* 28:365–372, 1970.
- ¹⁵Hingorani, R. V., P. P. Provenzano, R. S. Lakes, A. Escarcega, and R. Vanderby Jr. Nonlinear viscoelasticity in rabbit medial collateral ligament. *Ann. Biomed. Eng.* 32:306–312, 2004.
- ¹⁶Hunter, I. W., and R. E. Kearney. Generation of random sequences with jointly specified probability density and autocorrelation functions. *Biol. Cybern.* 47:141–146, 1983.
- ¹⁷Keshner, M. $1/f$ noise. *Proc. IEEE* 70:212–218, 1982.
- ¹⁸Kullmann, L., and J. Kertesz. Preferential growth: exact solution of the time-dependent distributions. *Phys. Rev. E Stat. Nonlin. Soft. Matter. Phys.* 63:051112, 2001.
- ¹⁹Maksym, G. N., and J. H. Bates. A distributed nonlinear model of lung tissue elasticity. *J. Appl. Physiol.* 82:32–41, 1997.
- ²⁰Maksym, G. N., R. E. Kearney, and J. H. Bates. Non-parametric block-structured modeling of lung tissue strip mechanics. *Ann. Biomed. Eng.* 26:242–252, 1998.
- ²¹Mead, J. Mechanical properties of lungs. *Physiol. Rev.* 41:281–330, 1961.
- ²²Mijailovich, S. M., D. Stamenovic, and J. J. Fredberg. Toward a kinetic theory of connective tissue micromechanics. *J. Appl. Physiol.* 74:665–681, 1993.
- ²³Murch, A., and R. Bates. Colored noise generation through deterministic chaos. *IEEE Trans. Circ. Syst.* 37:608–613, 1990.
- ²⁴Press, W. Flicker noise in astronomy and elsewhere. *Comm. Astrophys.* 7:103, 1978.
- ²⁵Ravasz, E., A. L. Somera, D. A. Mongru, Z. N. Oltvai, and A. L. Barabasi. Hierarchical organization of modularity in metabolic networks. *Science* 297:1551–1555, 2002.
- ²⁶Shenoy, A. *Rheology of Filled Polymer Systems*. Dordrecht: Kluwer, 1999, pp. 79–84.
- ²⁷Speich, J. E., K. Quintero, C. Dosier, L. Borgsmiller, H. P. Koo, and P. H. Ratz. A mechanical model for adjustable passive stiffness in rabbit detrusor. *J. Appl. Physiol.* 101:1189–1198, 2006.
- ²⁸Suki, B., A. L. Barabasi, Z. Hantos, F. Petak, and H. E. Stanley. Avalanches and power-law behaviour in lung inflation. *Nature* 368:615–618, 1994.
- ²⁹Suki, B., and J. H. Bates. A nonlinear viscoelastic model of lung tissue mechanics. *J. Appl. Physiol.* 71:826–833, 1991.
- ³⁰West, B., and M. Schlesinger. On the ubiquity of $1/f$ noise. *Int. J. Modern Phys.* 3:795–819, 1989.
- ³¹Yuan, H., D. T. Westwick, E. P. Ingenito, K. R. Lutchen, and B. Suki. Parametric and nonparametric nonlinear system identification of lung tissue strip mechanics. *Ann. Biomed. Eng.* 27:548–562, 1999.